

RESEARCH

Open Access



Phosphatidylinositol promoted the proliferation and invasion of pituitary adenoma cells by regulating POU1F1 expression

Tongjiang Xu^{1†}, Xiaodong Zhai^{1†}, RuiWei Wang², Xiaoben Wu³, ZhiZhen Zhou⁴, MiaoMiao Shang¹, Chongcheng Wang⁵, Tengfei Qi⁵ and Wei Yang^{1*}

Abstract

Invasiveness of pituitary adenoma is the main cause of its poor prognosis, mechanism of which remains largely unknown. In this study, the differential proteins between invasive and non-invasive pituitary tumors (IPA and NIPA) were identified by TMT labeled quantitative proteomics. The differential metabolites in venous bloods from patients with IPA and NIPA were analyzed by untargeted metabolomics. Proteomic data showed that the top five up-regulated proteins were AD021, C2orf15, PLCXD3, HIST3H2BB and POU1F1, and the top five down-regulated proteins were AIPL1, CALB2, GLUD2, SLC4A10 and GTF2I. Metabolomic data showed that phosphatidylinositol (PI) was most remarkably up-regulated and melibiose was most obviously down-regulated. Further investigation demonstrated that PI stimulation increased the expression of PITPNM1, POU1F1, C2orf15 and LDHA as well as the phosphorylation of AKT and ERK, and promoted the proliferation, migration and invasion of GH3 cells, which were blocked by PITPNM1 knock-down. Inhibiting AKT phosphorylation reduced the expression of POU1F1, C2orf15 and LDHA in PI-stimulated cells while activating AKT increased their expression in PITPNM1-silencing cells, which was similar to the function of ERK. POU1F1 silencing suppressed the expression of LDHA and C2orf15. Luciferase report assay and ChIP assay demonstrated that POU1F1 positively regulated the transcription of LDHA and C2orf15. In addition, PI propelled the metastasis of GH3 cells in vivo, and elevated the expression of PITPNM1, POU1F1, C2orf15 and LDHA. These results suggested that elevated serum PI might contribute to the proliferation and invasion of pituitary adenoma by regulating the expression of PITPNM1/AKT/ERK/POU1F1 axis.

Keywords Metabolomic, Phosphatidylinositol, PITPNM1, Pituitary tumor, POU1F1, Proteomic

[†]Tongjiang Xu and Xiaodong Zhai contributed equally to this work.

*Correspondence:

Wei Yang

neurosurgeon_yw@163.com

¹ Department of Neurosurgery, Provincial Hospital Affiliated to Shandong First Medical University, Jinan, Shandong 250021, China

² Department of Anesthesiology, Provincial Hospital affiliated to Shandong First Medical University, Jinan, Shandong 250021, China

³ Department of Clinical Laboratory, Provincial Hospital affiliated to Shandong First Medical University, Jinan, Shandong 250021, China

⁴ Department of Neurosurgery, Weishan People's Hospital, Jining, Shandong 277600, China

⁵ Trauma Center, Provincial Hospital Affiliated to Shandong First Medical University, Jinan, Shandong 250021, China

Introduction

Pituitary adenoma (PA) is one of the most common primary brain tumors, accounting for approximately 15% of intracranial tumors [1]. Although pituitary adenomas are benign tumors, about 30% of them actively invade surrounding tissues, which is called invasive pituitary tumor (IPA) [2]. Since IPA usually shows large size and invasive growth, drugs and radiotherapy are partially or completely ineffective, resulting in high mortality [3]. Therefore, it is necessary to explore the molecular mechanism of IPA, which contributes to the early detection and improves the survival rate of patients.



Untargeted metabolomics could provide a rapid and wide identification of differential metabolites among different pathological conditions. Metabolic disorder has recently been associated with tumor progression. Pituitary adenoma cells have been demonstrated to undergo remarkable metabolic reprogramming for aberrant hormone secretion [4], which might be reflected by serum metabolome. However, the serum metabolic difference between IPA and non-invasive pituitary tumor (NIPA) remains largely unknown.

The difference in serum metabolomics is attributed to the metabolic reprogramming of tumors, which in turn acts on the tumor cells to support cell proliferation, migration and invasion [5]. For instance, vigorous glycolysis provides energy for rapid growth of tumors [6]. The elevated lipid metabolism is implicated in tumor proliferation, metastasis and chemoresistance [7, 8]. Thus, the serum metabolic changes should be closely correlated to the difference of tumor proteomics.

In this study, we examined the metabonomic and proteomic differences between IPA and NIPA. The metabonomic results showed that the levels of phosphatidylinositol were significantly increased in the serums from patients with invasive pituitary tumors.

Combined with proteomic results, increased phosphatidylinositol was associated with the up-regulation of PITPNM1, IRS4, HLA-DPA1 and down-regulation of ACTG1, PFN1, PGAP1, ATG3, CAMK2G, ARHGEF12. Exposure of GH3 cells to phosphatidylinositol notably promoted cell invasion and the expression of PITPNM1, POU1F1 and C2orf15. Further investigation confirmed that the expression of PITPNM1, POU1F1 and C2orf15 were remarkably higher in IPA than that in NIPA. These results suggested that the elevated serum phosphatidylinositol might promote pituitary adenoma cells invasion by increasing the expression of PITPNM1, POU1F1 and C2orf15.

Results

Proteomic analysis of NIPA and IPA tissues

Based on the preoperative imaging, intraoperative findings and postoperative pathological diagnosis, 5 patients with IPA and 5 patients with NIPA were selected according to Hardy-Wilson and Knosp classification (Fig. 1A). Invasive pituitary tumor (IPA) and non-invasive pituitary tumor (NIPA) TMT labeled proteomics data were qualified and quantified using Maxquant software. Differential expression over 1.2-fold change and p value less

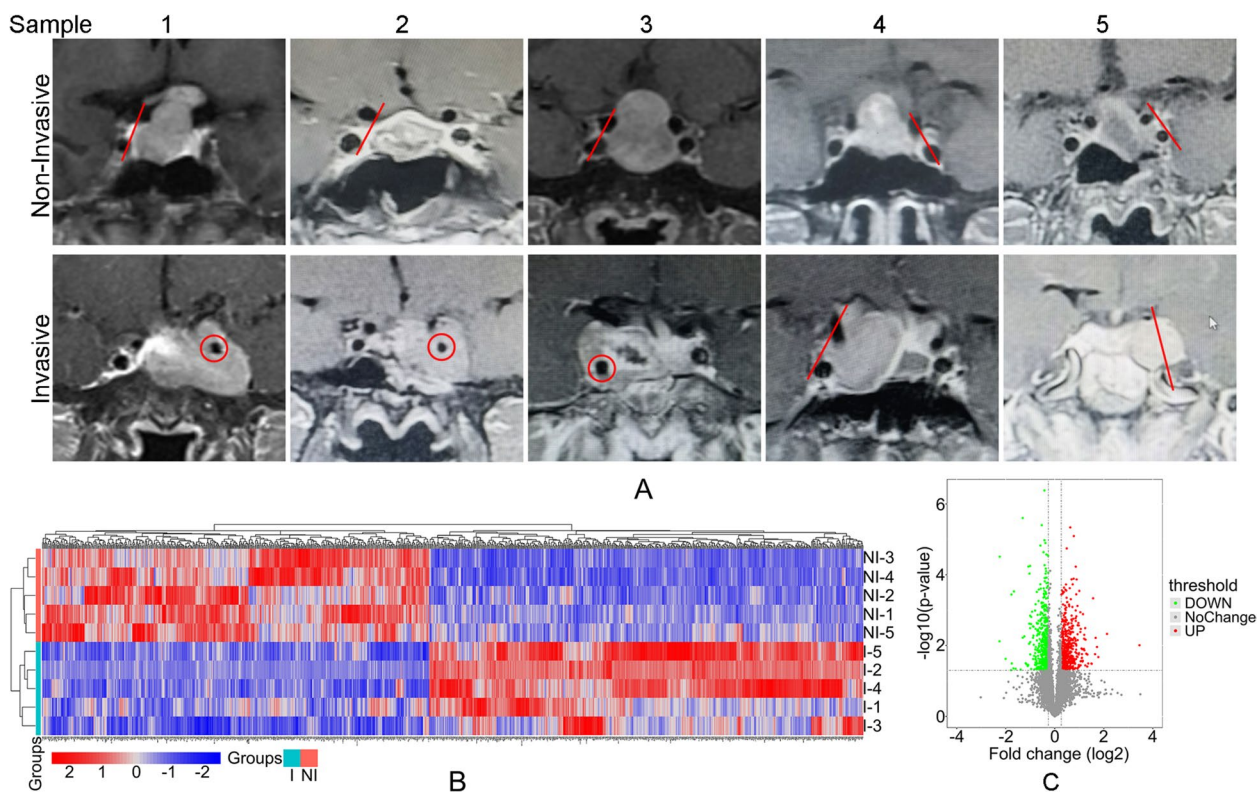


Fig. 1 Proteomic analysis of NIPA and IPA tissues. **A** The preoperative imaging of IPA and NIPA. **B** Cluster analysis of differential proteins between IPA and NIPA tissues. **C** Volcanic map of differential proteins between IPA and NIPA tissues

than 0.05 were considered as significant difference. The results showed that, compared with NIPA group, there were 948 differential proteins in IPA group, including 504 up-regulated proteins and 444 down-regulated proteins. Cluster analysis of these differentiated proteins was performed, and the results were shown in Fig. 1B. Volcano Plot was drawn using fold change of protein and p value by t-test, the results were shown in Fig. 1C, suggesting significant difference between the data from NIPA and IPA samples. The differentiated proteins were classified according to their genetic properties annotated by Gene ontology (GO) (Fig. 1s-A), including biological process (Fig. 1s-B), cell component (Fig. 1s-C) and molecular function (Fig. 1s-D). The KEGG enrichment analysis showed that these differentiated proteins were mainly involved in metabolic pathways (Fig. 2s). The top five up-regulated proteins were AD021, C2orf15, PLCXD3, HIST3H2BB and POU1F1, and the top five down-regulated proteins were AIPL1, CALB2, GLUD2, SLC4A10 and GTF2I (Fig. 2A). Among these proteins, POU1F1 regulates growth hormone synthesis, secretion and action (Fig. 2B), which is associated with PA progression.

Metabonomic analysis of venous blood from patients with NIPA and IPA

A total of 22 different metabolites were identified between serum from NIPA and IPA. The ion peak data of tested samples and QC samples were handled using unit variance scaling and analyzed by PCA, and the results were shown in Fig. 3A. The data of QC samples are closely clustered, indicating that the repeatability of metabonomic analysis is favorable and differences of metabolic spectra can reflect the biological variation among samples. The relationship between metabolite level and sample type was analyzed by PLS-DA, and the results were shown in Fig. 3B. The values of R2 and

Q2 were 0.999 and 0.711, respectively, which suggested that the model was stable and reliable. In order to evaluate the rationality of candidate metabolites, and display the relationship between samples and the differences of metabolites levels, hierarchical clustering was performed using the levels of differential metabolites and sample types, and the results were shown in Fig. 3C, suggesting that the level of phosphatidylinositol was notably higher in serum from patients with IPA than that in NIPA patients. The volcano plot generated by fold change and p value was shown in Fig. 3D. Figure 3E illustrated the fold change of differentiated metabolites in IPA serum compared with NIPA serum. Among these metabolites, phosphatidylinositol was most remarkably up-regulated and melibiose was most obviously down-regulated (Fig. 3E). These metabolites were mainly involved in phosphatidylinositol signaling system, glycosylphosphatidylinositol and phosphatidylinositol transport (Fig. 3F). These results indicated that phosphatidylinositol mediated signaling might play a key role in the PA invasion.

Conjoint analysis of proteome and metabolomics

We further performed conjoint analysis of proteome and metabolomics. The results showed 17 common genes between proteome and metabolomics (Fig. 4A). Common KEGG signaling pathway contained phosphatidylinositol transport (Fig. 4B). Phosphatidylinositol was closely associated with the up-regulation of HLA-DPA1, IRS4, and PITPNM1. Phosphatidylinositol was also correlated to the down-regulation of CAMK2G, ARHGEF12, PFN1, ACTG1, PGAP1 and ATG3 (Fig. 4C). Considering that PITPNM1 controls phosphatidylinositol transport, we speculated that elevated PITPNM1 expression in IPA tissue contributed to intracellular transport of phosphatidylinositol, which triggered intracellular signaling.

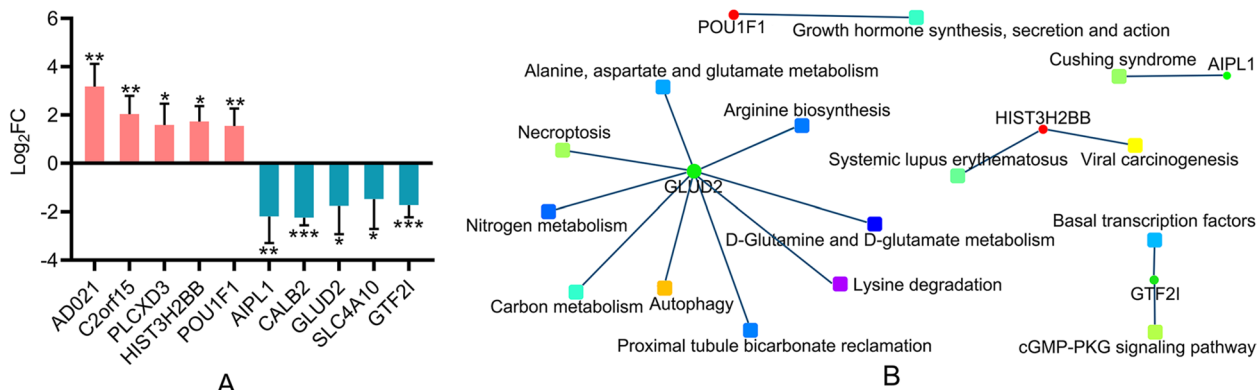


Fig. 2 Interaction network of the top five up-regulated and down-regulated proteins. **A** The fold changes of top five up-regulated and down-regulated proteins. *, $p < 0.05$ vs NIPA; **, $p < 0.01$ vs NIPA; ***, $p < 0.0001$ vs NIPA. **B** Interaction network of POU1F1, AIPL1, HIST3H2BB, GLUD2 and GTF2I

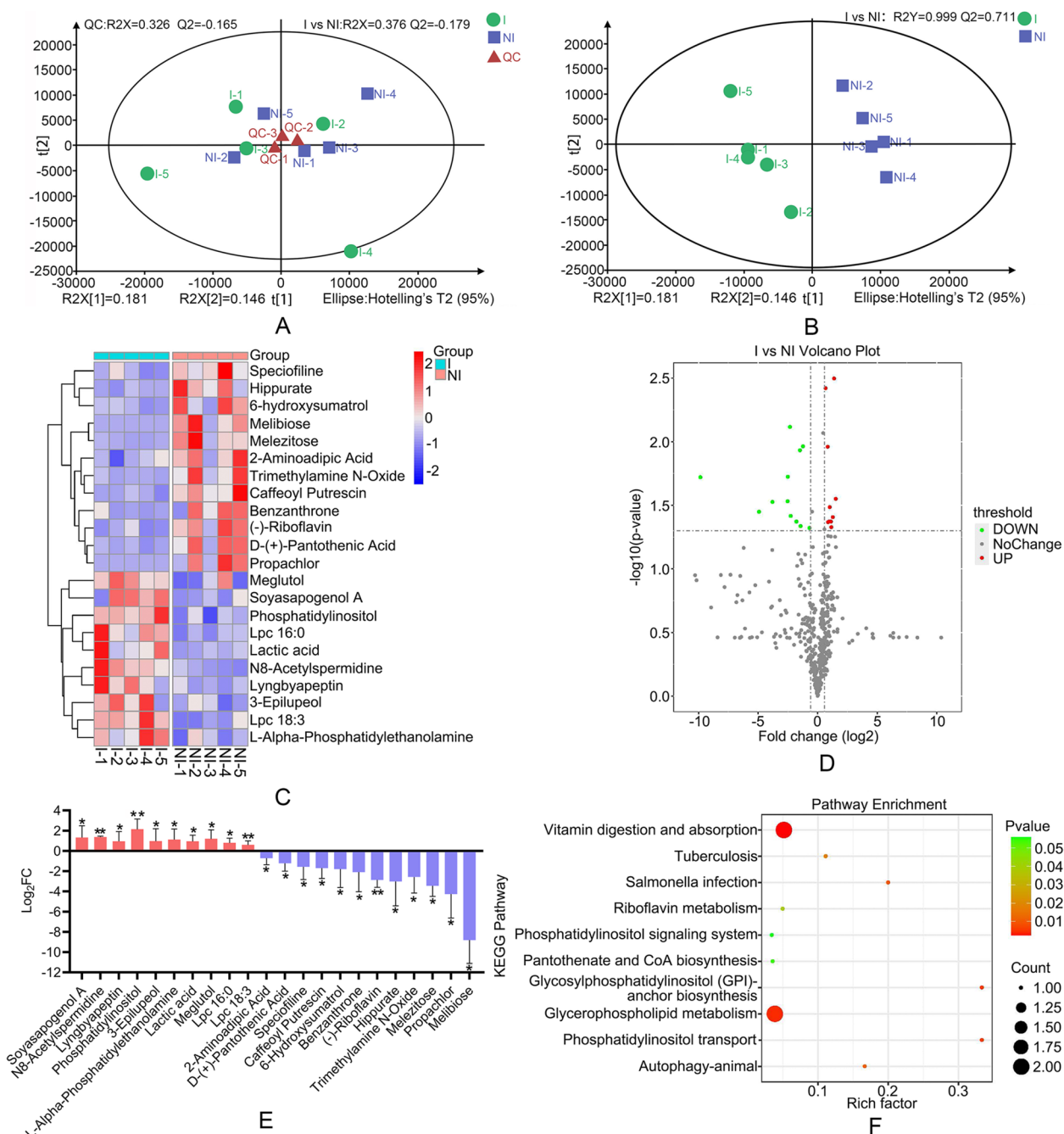


Fig. 3 Metabonomic analysis of venous blood from patients with NIPA and IPA. **A** PCA score of IPA compared to NIPA. **B** PLS-DA of IPA compared to NIPA. **C** Hierarchical clustering results of metabolites with significant differences. **D** Volcanic map of metabolites with significant differences. **E** The fold changes of significantly differential metabolites. *, $p < 0.05$ vs NIPA; **, $p < 0.01$ vs NIPA; ***, $p < 0.0001$ vs NIPA. **F** KEGG enrichment analysis of metabolic pathway implicated significantly differential metabolites

Proteomic analysis of phosphatidylinositol stimulated GH3 cells

We next analyzed the differential proteins expression of GH3 cells in presence or absence of phosphatidylinositol (PI). The results were shown in Fig. 5A. Volcano Plot

based on fold change of protein and p value was shown in Fig. 5B. The venn diagram was drawn by comparing the differential proteins from tissue and cell proteome (Fig. 5C). There were 20 common differential proteins, including PITPNM1, POU1F1 and C2orf15 (Fig. 5C).

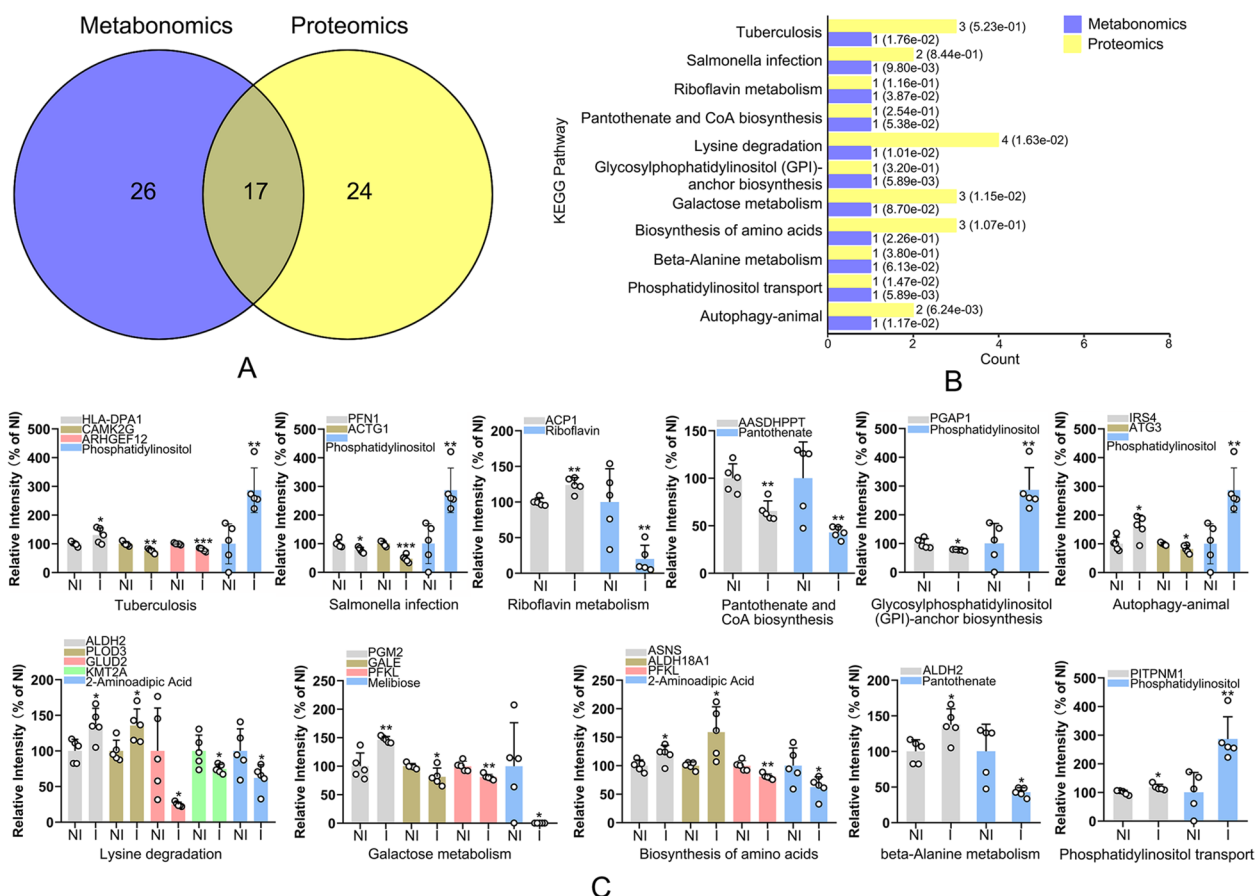


Fig. 4 Conjoint analysis of proteome and metabolomics. **A** Venn diagram of differential proteins involved in proteomics and metabolomics. **B** The common KEGG pathway of proteomics and metabolomics. **C** The correlation between differential proteins and metabolites. *, $p < 0.05$ vs NI group; **, $p < 0.01$ vs NI group; ***, $p < 0.001$ vs NI group

These results suggested that PI might promote IPA cells invasion by regulating the expression of PITPNM1, POU1F1 and C2orf15.

Phosphatidylinositol promoted pituitary adenoma cell proliferation, migration and invasion

Immunohistochemical analysis illustrated that the expression of PITPNM1, POU1F1 and C2orf15 in IPA tissues were notably higher than that in NIPA tissues (Fig. 6A). These results suggested that PI indeed promoted IPA cells invasion by elevating PITPNM1, POU1F1 and C2orf15. We further examined the effect of phosphatidylinositol (PI) on pituitary adenoma cell proliferation and invasion. The results suggested that, exposure of GH3 cells and primary pituitary adenoma cells (PPAC) to PI significantly promoted cell proliferation in a dose- and time-dependent manner, reaching to a peak at the dose of 100 $\mu\text{g/ml}$ (Fig. 6B and C). Transwell assay demonstrated that PI increased the invasion and migration of GH3 cells and PPAC (Fig. 6D and E). Further

investigation showed that PI induced the expression of PITPNM1, POU1F1, C2orf15 and LDHA as well as the phosphorylation of AKT and ERK (Fig. 6F).

PITPNM1 was required for PI-induced POU1F1 expression by regulating the phosphorylation of AKT and ERK

To test the role of PITPNM1 in PI-induced signaling transduction, the knockdown of PITPNM1 was performed. The results showed that PITPNM1 knockdown blocked PI-induced expression of POU1F1, C2orf15 and LDHA as well as the phosphorylation of AKT and ERK (Fig. 7A). As expected, PITPNM1 knockdown suppressed the invasion and migration of GH3 cells exposed to PI (Fig. 7B and C). Overexpression of PITPNM1 in PITPNM1-depleting cells recovered the expression of POU1F1, C2orf15 and LDHA as well as the phosphorylation of AKT and ERK (Fig. 7D). Meantime, PITPNM1 overexpression accelerated the invasion and migration of GH3 cells (Fig. 7E and F). MK2206, an inhibitor targeted AKT phosphorylation,

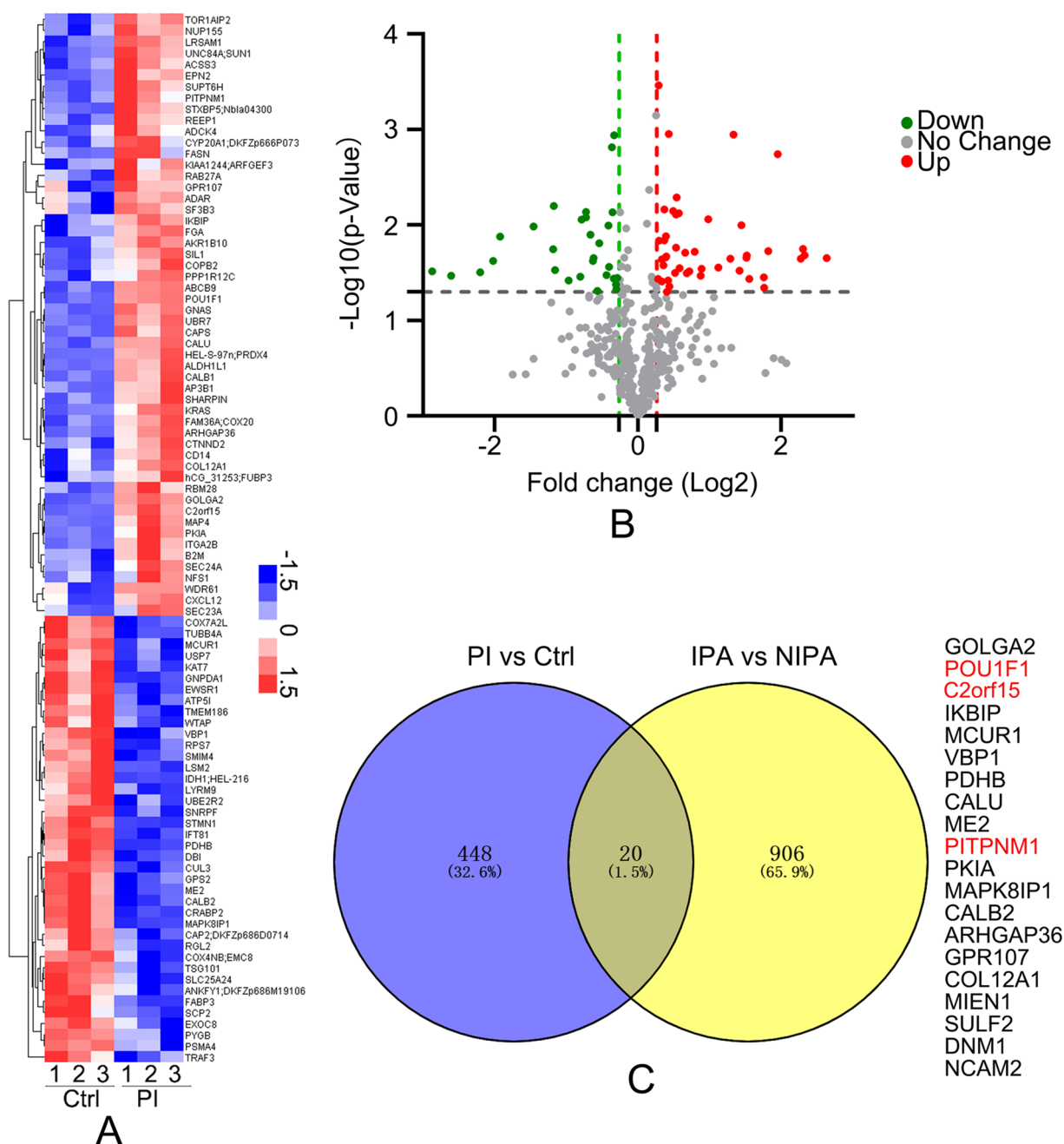


Fig. 5 Proteomic analysis of phosphatidylinositol stimulated GH3 cells. **A** Cluster analysis of differential proteins between GH3 cells and GH3 cells-treated with phosphatidylinositol. **B** Volcanic map of differential proteins between GH3 cells and GH3 cells-treated with phosphatidylinositol. **C** Venn diagram of differential proteins from IPA tissues and GH3 cells-treated with phosphatidylinositol

remarkably reduced PI-induced the expression of POU1F1 and C2orf15, and slightly inhibited PI-induced LDHA expression (Fig. 7G), whereas SC79 (an activator of AKT) notably increased the expression of POU1F1 and C2orf15 in PITPNM1-silencing cells (Fig. 7G), which were similar to ERK inhibition by

U0126 and activation by TBHQ, respectively (Fig. 7H). Intriguingly, whatever activation and inhibition of AKT or ERK did not affect the expression of PITPNM1. These results suggested that PITPNM1 was required for PI-induced POU1F1 expression by regulating the phosphorylation of AKT and ERK.

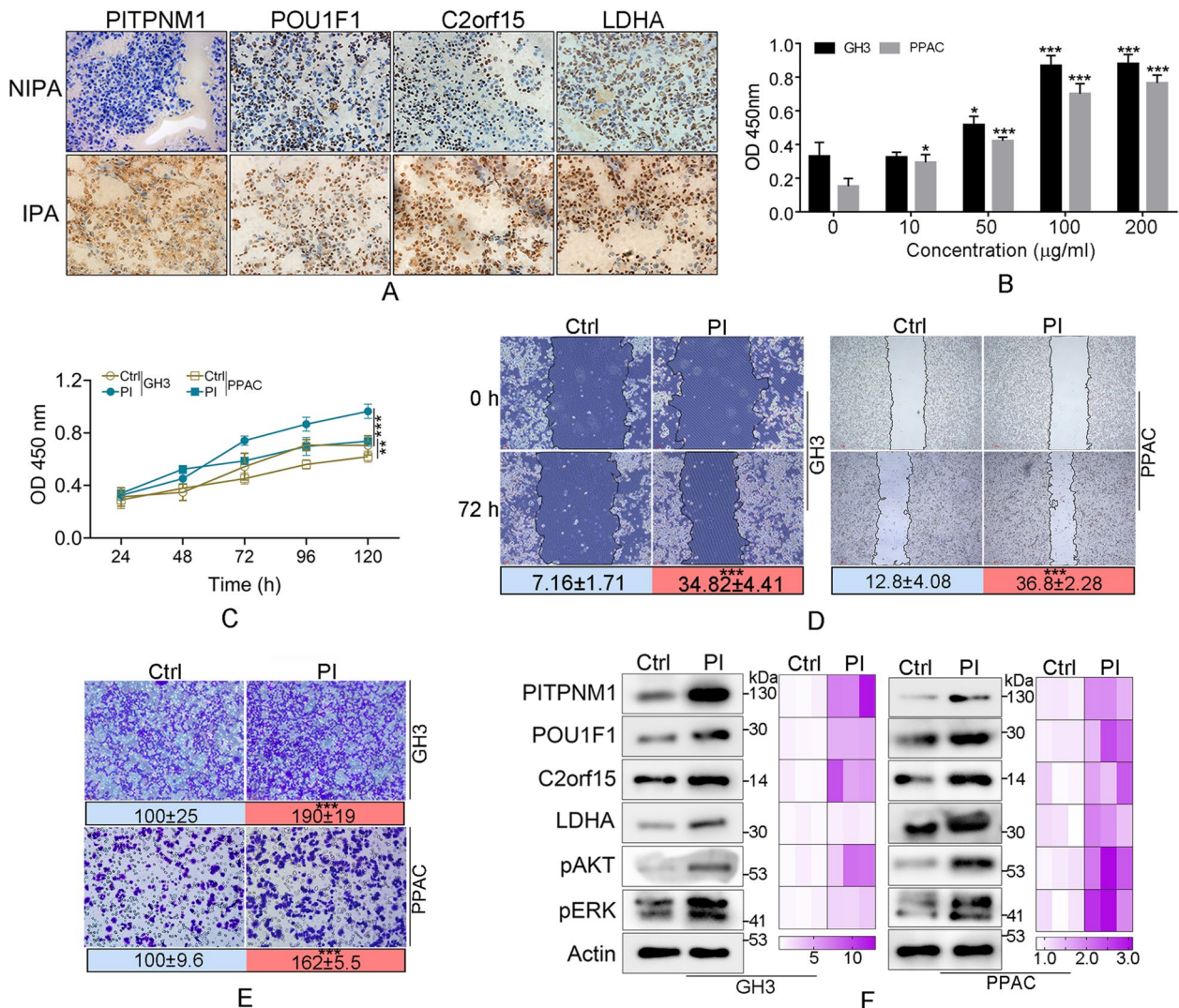


Fig. 6 The effect of phosphatidylinositol on the proliferation of invasion of pituitary adenoma cells and expression of PITPNM1, POU1F1 and C2orf15. **A** The expression of PITPNM1, POU1F1, C2orf15 and LDHA in IPA and NIPA tissues. **B** The primary pituitary adenoma cells (PPAC) and GH3 cells were exposed to the different concentration of phosphatidylinositol for 72 h. CCK8 assay was performed to determine the cell viability. **C** GH3 cells and PPAC were treated with 100 µg/ml phosphatidylinositol for indicated time. CCK8 assay was performed to determine the cell viability. **D** Scratch assay was performed to determine the effect of phosphatidylinositol on cell migration. **E** Transwell assay was performed to determine the effect of phosphatidylinositol on cell invasion. **F** After treatment with phosphatidylinositol, western blot analysis was performed to determine the expression of PITPNM1, POU1F1, C2orf15 and LDHA. ***, $p < 0.001$

POU1F1 positively regulated the transcription of C2orf15 and LDHA

We next examined the role of POU1F1 on the expression of C2orf15 and LDHA. The results showed that POU1F1 knockdown restrained the expression of C2orf15 and LDHA (Fig. 8A), and reduced the invasive capability of GH3 cells (Fig. 8B). However, C2orf15 knockdown did not affect the expression of POU1F1 and LDHA (Fig. 8C), but attenuated the invasion of GH3 cells (Fig. 8D). Similarly, LDHA knockdown did not affect the expression of POU1F1 and C2orf15 (Fig. 8E), but also decreased the

GH3 cells invasion (Fig. 8F). ChIP assay demonstrated that POU1F1 positively regulated the transcription of LDHA, which did not affect by PI treatment, consistent with the results from luciferase reporter assay (Fig. 8G and H). ChIP assay also confirmed that POU1F1 could bind to the site1 and site2 of C2orf15 promoter, which were enhanced by PI treatment (Fig. 8I), consistent with the results from luciferase reporter assay (Fig. 8J). These results suggested that POU1F1 positively regulated the transcription of C2orf15 and LDHA, especially, PI treatment notably enhanced the transcriptional activity of POU1F1 in C2orf15.

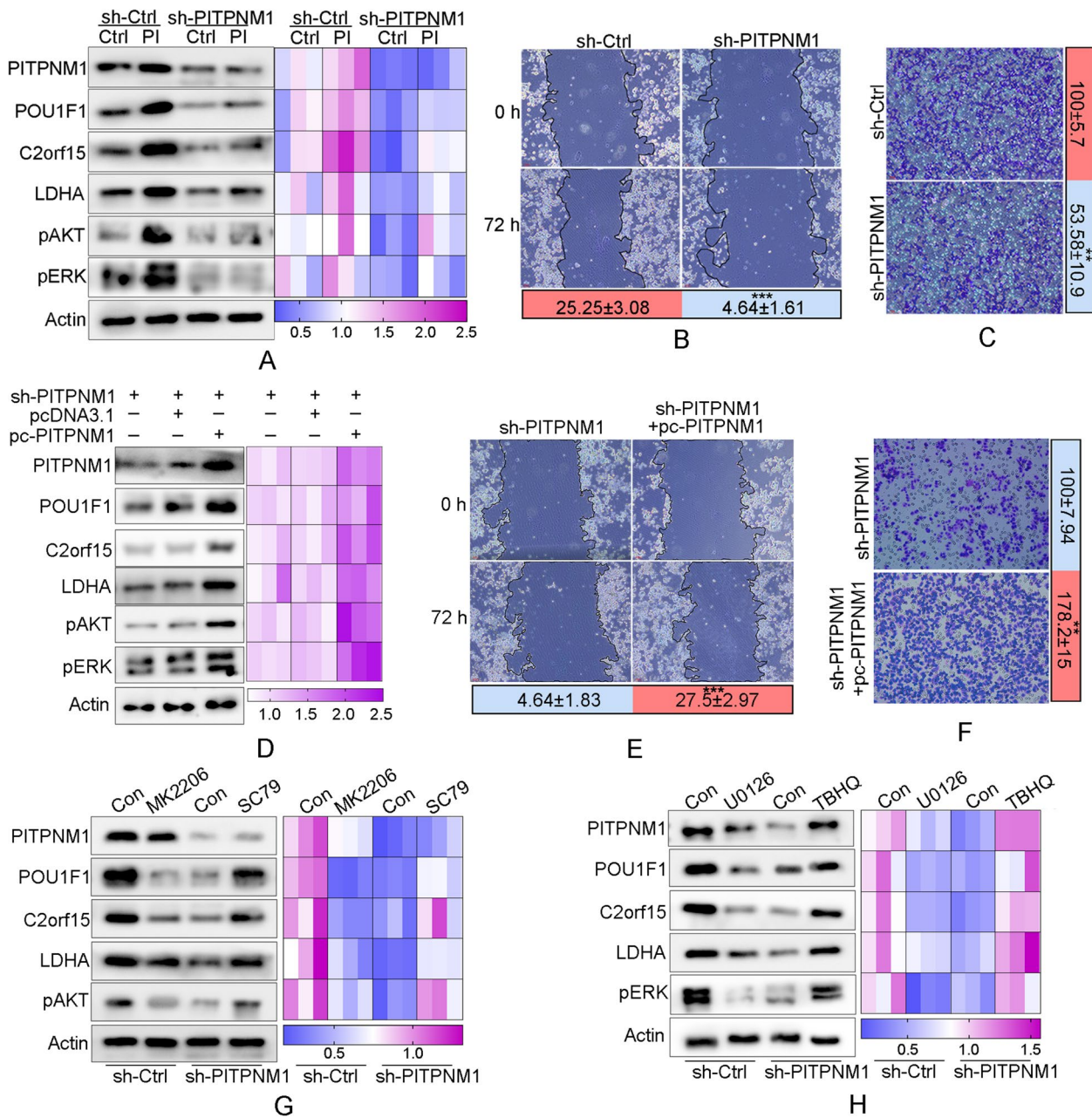


Fig. 7 PI-induced PITPNM1 was required for the expression of POU1F1, C2orf15 and LDHA via the phosphorylation of AKT (pAKT) and ERK (pERK). **A** The effect of PITPNM1 knockdown on PI-induced the expression of POU1F1, C2orf15 and LDHA as well as the phosphorylation of AKT and ERK. Western blot analysis was used to determine the protein expression. **B** The effect of PITPNM1 knockdown on PI-induced migration of GH3 cells. **C** The effect of PITPNM1 knockdown on PI-induced invasion of GH3 cells. **D** The effect of PITPNM1 overexpression in the PITPNM1-depleting cells on the expression of PITPNM1, POU1F1, C2orf15 and LDHA as well as the phosphorylation of AKT and ERK. **E** The effect of PITPNM1 overexpression in the PITPNM1-depleting cells on the cell migration. **F** The effect of PITPNM1 overexpression in the PITPNM1-depleting cells on the cell invasion. **G** The effect of AKT activation and inhibition on PI-induced expression of PITPNM1, POU1F1, C2orf15 and LDHA. **H** The effect of ERK activation and inhibition on PI-induced expression of PITPNM1, POU1F1, C2orf15 and LDHA. **, $p < 0.01$; ***, $p < 0.001$

PI accelerated the lung metastasis of PA cells in vivo

We finally investigated the effect of PI on the migration and invasion of PA cells in vivo. Tissue fluorescence imaging demonstrated that PI treatment

accelerated the lung metastasis of GH3 cells (Fig. 9A). Furthermore, PI treatment increased the expression of PITPNM1, POU1F1 and C2orf15, while had no obvious effect on LDHA expression (Fig. 9B and C).

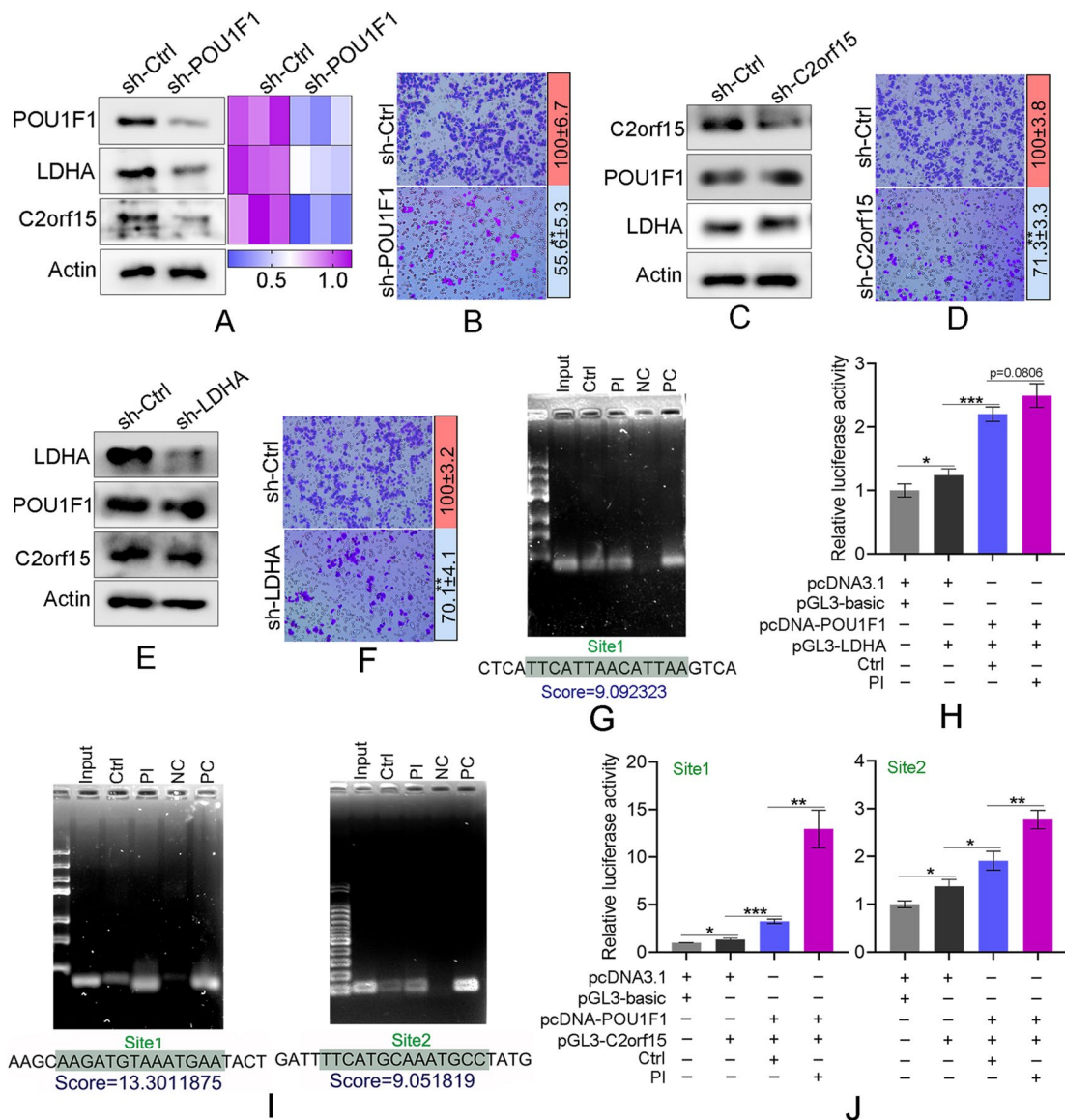


Fig. 8 POU1F1 positively regulated the transcription of C2orf15 and LDHA. **A** The effect of POU1F1 knockdown on the expression of C2orf15 and LDHA. **B** The effect of POU1F1 knockdown on the invasion of GH3 cells. **C** The effect of C2orf15 knockdown on the expression of POU1F1 and LDHA. **D** The effect of C2orf15 knockdown on the invasion of GH3 cells. **E** The effect of LDHA knockdown on the expression of POU1F1 and C2orf15. **F** The effect of LDHA knockdown on the invasion of GH3 cells. **G** Chromatin immunoprecipitation (ChIP) assay was performed to determine the bind of POU1F1 to the promoter of LDHA. **H** Luciferase reporter assay was performed to determine the activity of POU1F1 on LDHA transcription. **I** ChIP assay was performed to determine the bind of POU1F1 to the promoter of C2orf15. **J** Luciferase reporter assay was performed to determine the activity of POU1F1 on C2orf15 transcription. *, $p < 0.05$; ***, $p < 0.001$. **, $p < 0.01$; ***, $p < 0.001$

Discussion

In this study, the peripheral blood of patients with invasive and non-invasive pituitary tumors were collected, and metabonomic analysis was performed. The results showed that the serum phosphatidylinositol (PI) level of patients with invasive pituitary tumors was significantly elevated. PI is an important phospholipid component in cell membrane, and the phosphorylation of its inositol

group directly regulates intracellular signal transduction. PI is first phosphorylated to PI(4)P by phosphatidylinositol 4-kinase PI4K, and PI(4)P is converted to PI(4, 5)P2 by phosphatidylinositol 5-kinase. PI(4, 5)P2 regulates a variety of cell events, including cytoskeletal reassembly, cell migration, and integrin-mediated cell adhesion [9–11]. Sustainable supplementation of PI could maintain cell order.

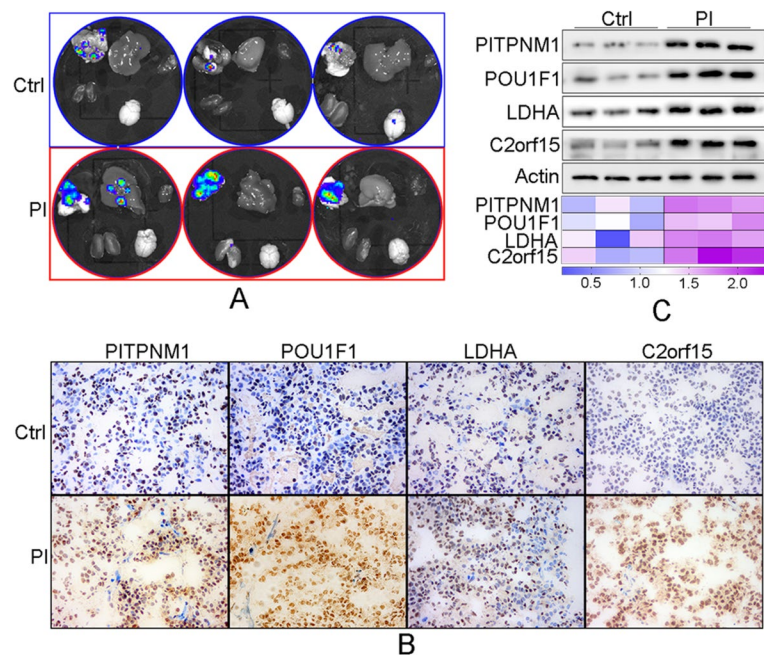


Fig. 9 PI accelerated lung metastasis of GH3 cells in vivo. **A** Nude mice were inoculated GH3 cells via tail vein, and were feed with normal diet or normal diet with oral administration of PI (120 mg/kg) for nine weeks, respectively. The tissues including lung, brain, liver, heart and kidney were detected using in vivo imaging system. **B** The expression of PITPNM1, POU1F1, C2orf15 and LDHA were determined by the immunohistochemical analysis. **C** The expression of PITPNM1, POU1F1, C2orf15 and LDHA were determined using western blot. *, $p < 0.05$

The transport of PI is regulated by phosphatidylinositol transporters (PITPs). A large number of studies have confirmed that PITPs play key roles in PI turnover and mediate PI signaling pathway [12–14], which has been implicated in tumor cells proliferation, invasion and metastasis [15]. PITPNM1, as a Class II PITPs, regulates the phosphorylation of protein kinases PKB, AKT and ERK in different types of tumor cells, and participates in their invasion and metastasis [16]. PITPNM1 was significantly up-regulated during invasion and metastasis of breast epithelial carcinoma, and inhibition of PITPNM1 significantly reduced lung metastasis of breast cancer [17]. Furthermore, PITPNM1 expression was also significantly up-regulated in human breast cancer samples [17]. Our results demonstrated that PITPNM1 knockdown blocked PI-induced the expression of POU1F1, C2orf15 and LDHA as well as the phosphorylation of AKT and ERK. These results suggest that accumulated PI should be transported to cell membrane by PITPNM1, supporting the cascade amplification of intracellular signals.

Following the metabonomic analysis, we analyzed proteomic differences between IPA and NIPA tissues. The results showed that PITPNM1 expression was significantly up-regulated in IPA tissues. Thus, we speculated that elevated serum PI induced PITPNM1 expression in pituitary tumor cells, which further increase the accumulation of PI on cell membrane. The phosphorylation of

PI promoted the generation of intracellular second messenger PIP2 and PIP3, enhancing the intracellular signals, which accelerated the invasion of pituitary tumor cells [18]. PI3K controls phosphorylation of PIP2 to PIP3, and has been well-known in tumor proliferation and metastasis [19]. ERK is another important protein kinase independent of PI3K-AKT. As a PI transporter, PITPNM1 up-regulation promotes epithelial-mesenchymal transformation (EMT) by activating PI3K-AKT and ERK signaling pathways, and knockdown of PITPNM1 inhibits breast cancer invasion and lung metastasis in vivo [15]. Our results confirmed that PI promoted the migration and invasion of pituitary tumor cells in vitro, and accelerated the lung metastasis of pituitary tumor cells in vivo. In addition, PI triggered the phosphorylation of AKT and ERK. These results suggest that PI should be involved in invasion and metastasis of pituitary tumors by regulating PI3K-AKT and ERK signaling pathways.

We further analyzed the effects of PI on GH3 proteome. The results showed that PI not only induced up-regulation of PITPNM1, but also significantly promoted the expression of POU1F1 and C2orf15. Combined with the proteomics analysis of pituitary tumors, PITPNM1, POU1F1 and C2orf15 were significantly upregulated in invasive pituitary tumor tissue and PI-stimulated GH3 cells, suggesting that PI might induce the expression of POU1F1 and C2orf15 by regulating PITPNM1. In deed,

exposure of GH3 cells to PI increased the expression of POU1F1 and C2orf15, which were blocked by PITPNM1 knockdown.

POU1F1 is pituitary specific positive transcription factor 1, also known as PIT-1, which plays a key role in the differentiation of anterior pituitary cells in mammals and is a transcriptional activator of pituitary gene expression [20]. POU1F1 is up-regulated in human tumorigenic breast cells [21, 22]. Knockout or overexpression of POU1F1 in human breast cancer cell lines induces significant phenotypic changes and regulates the expression of Snai1 [23]. In nude mice, POU1F1 overexpression promotes tumor growth and lung metastasis [23]. In patients with invasive ductal carcinoma of breast, POU1F1 was significantly correlated with Snai1 expression [23]. In addition, the up-regulation of POU1F1 expression was significantly independently correlated with the occurrence of distant metastasis [24, 25]. These results suggest that the up-regulation of POU1F1 expression is closely related to tumor invasion and metastasis.

Studies have shown that FGFR2 regulates Mre11 expression and DNA double-strand damage repair through MEK-ERK-POU1F1 pathway [26], and EGF regulates POU1F1 expression through PKC ϵ -ERK pathway [27], indicating that ERK activation might increase POU1F1 expression. Considering that PI is involved in the activation of ERK, it is likely that PI promotes the POU1F1 expression and drives the invasion and metastasis of pituitary tumor cells by activating ERK. Our results verified that activation of ERK elevated the expression of POU1F1 in despite of PITPNM1 knockdown while ERK inhibition remarkably reduced POU1F1 expression in the presence of PI. These results indicated that ERK activation was key for PI-induced POU1F1 expression.

POU1F1, as a transcription factor, has a specific recognition site of 5'-TAAAT-3', which activates the transcription of growth hormone and prolactin genes [28]. Furthermore, POU1F1 activates the expression of lactate dehydrogenase (LDHA), induces breast cancer metabolic reprogramming and promotes breast cancer progression [29]. Our results also confirmed that serum level of lactate in IPA patients was elevated, suggesting that PI-induced POU1F1 expression might be responsible for increasing serum lactate. Further investigation revealed that POU1F1 positively regulated the transcription of LDHA.

In summary, our results suggested that the increased serum PI in patients with IPA promoted PITPNM1 expression, which in turn increased the accumulation and intracellular transport of PI, activating AKT and ERK. The phosphorylation of AKT and ERK promoted POU1F1 expression. POU1F1 positively regulated the transcription of LDHA and C2orf15, elevating serum

level of lactate, which should be responsible for invasion and metastasis of pituitary tumor (Fig. 10).

Materials and methods

Materials

Anti-PITPNM1 for IHC was purchased from Bioss (Beijing, China); anti-POU1F1 and anti-C2orf15 were purchased from Bioss (Beijing, China); anti-GAPDH was purchased from Proteintech (Proteintech group Inc, Rosemont, US). RIPA lysis buffer was purchased from Solarbio. DMEM medium and fetal bovine serum were purchased from Gibco Life Technologies (Grand Island, NY, USA). All experiments were performed with mycoplasma-free cells.

Preparation of specimens and ethics approval

The patients with pituitary adenoma were recruited from Shandong Provincial Hospital Affiliated to Shandong First medical University. Based on the preoperative imaging, intraoperative findings and postoperative pathological diagnosis, 5 patients with IPA and 5 patients with NIPA were selected according to Hardy-Wilson and Knosp classification. Venous bloods and pituitary adenoma tissues were collected for metabolomic and proteomic analysis, respectively. This study has been approved by the Ethics Committee of Shandong Provincial Hospital Affiliated to Shandong First medical University, and written informed consent was obtained from every participant.

Metabolite extraction

100 μ l of venous blood was mixed with 100 μ l of pre-cold water and 800 μ l of pre-cold methanol/acetonitrile (1:1, v/v) after thawing at 4 $^{\circ}$ C, followed by ultrasound in ice bath for 60 min, and incubation at -20 $^{\circ}$ C for 1 h to precipitate protein. After centrifugation at 16000 g for 20 min at 4 $^{\circ}$ C, the supernatant is dried in a high speed vacuum centrifuge. 100 μ l of acetonitrile-water solution (1:1, v/v) was added for redissolution, and underwent centrifugation at 14000 g for 15 min at 4 $^{\circ}$ C. The supernatant was collected for Mass Spectrometry analysis.

LC-MS analysis

The samples were detected by Agilent 1290 Infinity LC ULTRA high performance liquid chromatography (UHPLC). The metabolites were separated by HILIC column, the injection volume was 5 μ l, and the column temperature was set as 25 $^{\circ}$ C. and the flow rate was 0.3 mL/min. The mobile phase A was water containing 25 mM ammonium acetate and 25 mM ammonia water. The mobile phase B was acetonitrile. The gradient elution procedure was as follows: 95% of B was maintained at 0 to 0.5 min, and then B was linearly changed from

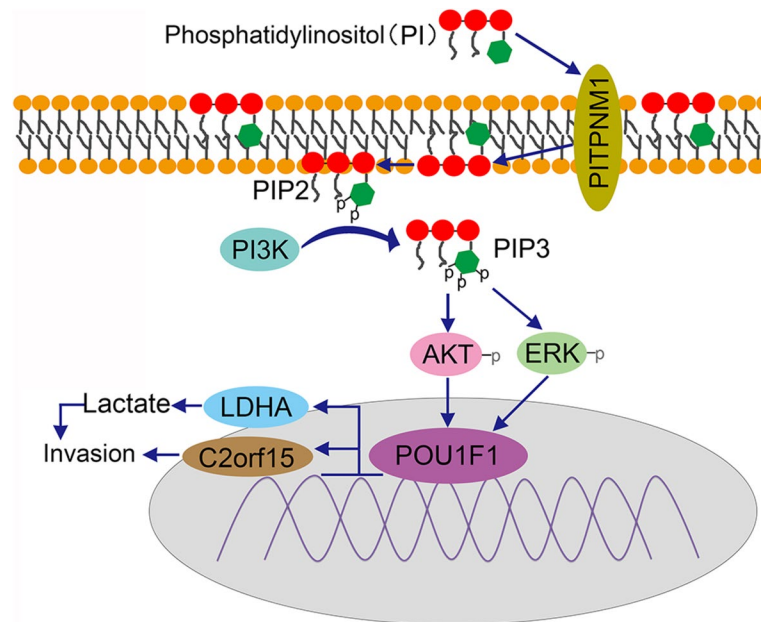


Fig. 10 The putative mechanism of phosphatidylinositol-mediated in pituitary tumor cells invasion

95 to 65% at 0.5 to 7 min; At 7 to 9 min, B was linearly changed from 65 to 40%, and 40% of B was remained at 9 to 10 min; At 10 to 11.1 min, B was linearly changed from 40 to 95%, and 95% of B was maintained at 11.1 to 16 min. QC samples were detected to evaluate the stability of the system and the reliability of experimental data. After being separated by UHPLC, the samples were analyzed by Triple TOF 5600 mass spectrometer (AB SCIEX).

Proteomic analysis

Pituitary adenoma tissues were ground in liquid nitrogen, and were mixed with 600 µl SDT, followed by boiling water bath for 5 min, ultrasound for 2 min, and boiling water bath for 5 min. After centrifugation at 15,000 g for 20 min at 4 °C, the supernatants were collected and protein concentration was quantified by BCA method. Enzymatic hydrolysis of protein (300 µg) from every sample was performed by Trypsin (0.15 µg/µl in TEAB buffer) and formed peptides were desalted by C18 cartridge. 100 µg of peptides were labeled using TMT labeling kit according to the manufacturer’s instructions (Thermo Fisher). Equal amount of labeled peptides in each group were mixed and dried, followed fractionation by High pH reversed-phase chromatography. The samples were collected and combined into 10 groups, and were dried and redissolved in 0.1% FA for LC–MS analysis. Peptides were separated using Easy-nLC 1200 chromatography system (Thermo Scientific) and analyzed by Q-Exactive HF-X mass spectrometer (Thermo Scientific).

CCK8 assay

The primary pituitary adenoma cells were prepared according to the previous description [30]. The rat GH3 pituitary adenoma cell line was obtained from the American Type Culture Collection (Manassas, VA). Cells were cultured in DMEM medium supplemented with 15% horse serum and 5% FBS, 100 U/mL penicillin, 100 U/mL streptomycin and 0.03% L-glutamine at 37 °C in 5% CO₂. GH3 cells were seeded at a density of 1×10⁴ cell/well in 96-well plate and cultured overnight, and then were treated with different concentration of phosphatidylinositol for 72 h or 100 µg/ml phosphatidylinositol for indicated time. CCK8 assay was performed to determine the cell viability.

Scratch assay

The GH3 cells were grown to the monolayer in 6-well plates, and a scratch was created using a pipette tip. After washed with PBS, the cells were cultured in complete medium containing 100 µg/ml phosphatidylinositol for 72 h. Images were captured using the olympus microscope (IX53).

Invasion assay

The GH3 1cells were seeded in DMEM medium in the upper chambers coated with matrigel coating (BD Biosciences, USA). DMEM medium containing 15% horse serum, 5% FBS and 100 µg/ml phosphatidylinositol was added into the lower chambers. After incubation for 48 h,

the cells invaded to the bottom membrane surface were visualized by DAPI staining.

Western blot analysis

The total protein was obtained using RIPA lysis buffer, and the concentration was measured using BCA method. Equal amount of protein was subjected to 10% SDS-PAGE electrophoresis, and was transferred to PVDF membrane. After blocking for 1 h with 5% nonfat milk at room temperature, the membrane was incubated in the antibodies of PITPNM1 (1:2000), POU1F1 (1:2000), C2orf15 (1:1000), pAKT (1:1000), pERK (1:1000) and Actin (1:2000) at 4 °C overnight, followed by incubation with HRP-coupled secondary antibodies at room temperature for 1 h. The protein bands were analyzed using the enhanced chemiluminescence method.

Immunohistochemistry

The tissues were fixed with paraformaldehyde overnight, followed by rehydration, paraffin embedding, section and dewaxing at room temperature. After antigen retrieval in EDTA solution using microwave treatment, the sections were incubated in 3% hydrogen peroxide, and were blocked using 10% rabbit serum. After incubating with primary antibodies and the HRP-labeled secondary antibodies, the sections were incubated in the fresh DAB solution and were counterstained using the hematoxylin. The images were visualized using an olympus microscope (IX53).

Chromatin Immunoprecipitation

The pituitary adenoma (PA) tissues were rinsed using the sterile PBS, and were then cut into small pieces with a size of 1 mm³ in serum-free DMEM medium. The tissue block was subjected to trypsinization for 30 min at 37 °C. After centrifugation at 1500 rpm for 5 min, the PA cells were collected and resuspended in DMEM medium containing 20% FBS in polylysine-coated 6-well plates.

Chromatin immunoprecipitation (ChIP) assay was performed using ChIP kit (Abcam, AB500) according to the instruction of manufacturer. The PA cells were harvested and resuspended in 1.1% formaldehyde for 10 min, followed by blocking using glycine. After lysis and ultrasound, the supernatant was obtained for DNA samples. The DNA samples were incubated with the indicated antibodies and microbeads for immunoprecipitation overnight. The DNA was purified and used as templates to amplify the target fragments (LDHA: Site1 F, 5'-TGGCTCCTTCCTGAGGCTAT-3'; Site1 R, 5'-CCAAAATTTCCTGAATTTTCTGAT-3'. C2orf15: Site1 F, 5'-TGCGAGCAACAATAAAGAT-3'; Site1 R, 5'-GCTTTCCCTGCCTTTACTGT-3'; Site2 F, 5'-TCATTTCTGAGCCTCTTTCT-3'), followed by analysis using agarose gel electrophoresis.

Luciferase reporter assay

The sequence containing POU1F1 binding sites, including site 1 of LDHA or site 1 and 2 of C2orf15, were amplified and linked into pGL3-Basic vector to construct pGL3-LDHA, pGL3-C2orf15-1 and pGL3-C2orf15-2, respectively. The open reading frame of POU1F1 was amplified and cloned into pcDNA3.1 plasmid to construct pcDNA3.1-POU1F1. 293 T cells were inoculated in 24-well plates at a density of 7×10^4 cells/well and cultured overnight. The cells were co-transfected with 250 ng pcDNA3.1-POU1F1, 250 ng pGL3-LDHA or pGL3-C2orf15, and pRL-TK plasmid using Lipofectamine 3000 (Roche). After 24 h of incubation, cellular lysates were harvested to detect luciferase activity using the Dual Luciferase assay system (Promega).

In vivo PA model

Six-week-old male BALB/c nude mice were used for in vivo PA model (Beijing Vital River Animal Center, Beijing, China), and were maintained under specific pathogen-free conditions. All procedures had been approved by laboratory Animal Ethics Committee of Shandong Provincial Hospital Affiliated to Shandong First Medical University. A total of 10 nude mice were inoculated 1×10^7 GH3 cells in 100 μ l sterile PBS via tail vein, which were randomly divided into two groups feed with normal diet or normal diet with oral administration of PI (120 mg/kg), respectively. After inoculation for nine weeks, mice were sacrificed and the tissues including lung, brain, liver, heart and kidney were detected using in vivo imaging system. The lung tissues were embedded in paraffin for HE and immunohistochemistry staining analysis.

Statistical analysis

All data were represented the mean \pm standard deviation from at least three independent experiments. The Differences between two groups were evaluated by t-test. The differences among multiple groups were evaluated by two-way ANOVA. The enrichment analysis of Gene ontology and KEGG were performed using Fisher's Exact Test. $P < 0.05$ was considered statistically significant. Statistical analysis was performed by GraphPad Prism 8.0.1 software package.

Supplementary Information

The online version contains supplementary material available at <https://doi.org/10.1186/s40170-024-00372-0>.

Supplementary Material 1.

Acknowledgements

Thanks to Dr. Yanliang Lin for his help in data analysis of proteome and metabolomics.

Authors' contributions

Wei Yang: Conceptualization, Methodology, Project administration. Tongjiang Xu and Xiaodong Zhai: Investigation, Writing—Original Draft. Xiaodong Zhai: Investigation, Validation. RuiWei Wang: Formal analysis. Xiaoben Wu: Resources, Funding acquisition. ZhiZhen Zhou: Visualization. MiaoMiao Shang: Writing—Review & Editing. Chongcheng Wang and Tengfei Qi: Performing in vivo experiments.

Funding

This study was supported by the Natural Science Foundation of Shandong Province (No. ZR2023MH271), the Foundation of Shandong Provincial Hospital (No. yw002), and the Clinical Medicine Science and Technology Innovation Project of JINAN (No. 202019020).

Data availability

No datasets were generated or analysed during the current study.

Declarations

Competing interests

The authors declare no competing interests.

Received: 17 July 2024 Accepted: 29 December 2024

Published online: 14 January 2025

References

- Mete O, Lopes MB. Overview of the 2017 WHO Classification of Pituitary Tumors. *Endocr Pathol.* 2017;28:228–43.
- Li J, Qian Y, Zhang C, Wang W, Qiao Y, Song H, et al. LncRNA LINC00473 is involved in the progression of invasive pituitary adenoma by upregulating KMT5A via ceRNA-mediated miR-502-3p evasion. *Cell Death Dis.* 2021;12:580.
- Ilie MD, Jouanneau E, Raverot G. Aggressive Pituitary Adenomas and Carcinomas. *Endocrinol Metab Clin North Am.* 2020;49:505–15.
- Feng J, Zhang Q, Zhou Y, Yu S, Hong L, Zhao S, et al. Integration of Proteomics and Metabolomics Revealed Metabolite-Protein Networks in ACTH-Secreting Pituitary Adenoma. *Front Endocrinol.* 2018;9:678.
- Zanotelli MR, Zhang J, Reinhart-King CA. Mechanoresponsive metabolism in cancer cell migration and metastasis. *Cell Metab.* 2021;33:1307–21.
- Liu J, Liu ZX, Wu QN, Lu YX, Wong CW, Miao L, et al. Long noncoding RNA AGPG regulates PFKFB3-mediated tumor glycolytic reprogramming. *Nat Commun.* 2020;11:1507.
- Bian X, Liu R, Meng Y, Xing D, Xu D, Lu Z. Lipid metabolism and cancer. *J Exp Med.* 2021;218:e20201606.
- Cao Y. Adipocyte and lipid metabolism in cancer drug resistance. *J Clin Investig.* 2019;129:3006–17.
- Marat AL, Haucke V. Phosphatidylinositol 3-phosphates-at the interface between cell signalling and membrane traffic. *EMBO J.* 2016;35:561–79.
- Katan M, Cockcroft S. Phosphatidylinositol(4,5)bisphosphate: diverse functions at the plasma membrane. *Essays Biochem.* 2020;64:513–31.
- Feng Z, Yu CH. PI(3,4)P(2)-mediated membrane tubulation promotes integrin trafficking and invasive cell migration. *Proc Natl Acad Sci U S A.* 2021;118:e2017645118.
- Nile AH, Tripathi A, Yuan P, Mousley CJ, Suresh S, Wallace IM, et al. PITPs as targets for selectively interfering with phosphoinositide signaling in cells. *Nat Chem Biol.* 2014;10:76–84.
- Ashlin TG, Blunsom NJ, Cockcroft S. Courier service for phosphatidylinositol: PITPs deliver on demand. *Biochim Biophys Acta.* 2021;1866: 158985.
- Kim S, Kedan A, Marom M, Gavert N, Keinan O, Selitrennik M, et al. The phosphatidylinositol-transfer protein Nir2 binds phosphatidic acid and positively regulates phosphoinositide signalling. *EMBO Rep.* 2013;14:891–9.
- Keinan O, Kedan A, Gavert N, Selitrennik M, Kim S, Karn T, et al. The lipid-transfer protein Nir2 enhances epithelial-mesenchymal transition and facilitates breast cancer metastasis. *J Cell Sci.* 2014;127:4740–9.
- Li H, Zhao X, Wen X, Zeng A, Mao G, Lin R, et al. Inhibition of miR-490-5p Promotes Human Adipose-Derived Stem Cells Chondrogenesis and Protects Chondrocytes via the PITPNM1/PI3K/AKT Axis. *Frontiers in cell and developmental biology.* 2020;8: 573221.
- Liu Z, Shi Y, Lin Q, Yang W, Luo Q, Cen Y, et al. Attenuation of PITPNM1 signaling cascade can inhibit breast cancer progression. *Biomolecules.* 2021;11:1265.
- Wu S, Chen M, Huang J, Zhang F, Lv Z, Jia Y, et al. ORAI2 Promotes Gastric Cancer Tumorigenicity and Metastasis through PI3K/Akt Signaling and MAPK-Dependent Focal Adhesion Disassembly. *Can Res.* 2021;81:986–1000.
- Chalhoub N, Baker SJ. PTEN and the PI3-kinase pathway in cancer. *Annu Rev Pathol.* 2009;4:127–50.
- Allensworth-James M, Banik J, Odle A, Hardy L, Lagasse A, Moreira ARS, et al. Control of the anterior pituitary cell lineage regulator POU1F1 by the stem cell determinant musashi. *Endocrinology.* 2021;162:bqaa245.
- Seoane S, Martinez-Ordonez A, Eiro N, Cabezas-Sainz P, Garcia-Caballero L, Gonzalez LO, et al. POU1F1 transcription factor promotes breast cancer metastasis via recruitment and polarization of macrophages. *J Pathol.* 2019;249:381–94.
- Martinez-Ordonez A, Seoane S, Cabezas P, Eiro N, Sendon-Lago J, Macia M, et al. Breast cancer metastasis to liver and lung is facilitated by Pit-1-CXCL12-CXCR4 axis. *Oncogene.* 2018;37:1430–44.
- Ben-Batalla I, Seoane S, Garcia-Caballero T, Gallego R, Macia M, Gonzalez LO, et al. Deregulation of the Pit-1 transcription factor in human breast cancer cells promotes tumor growth and metastasis. *J Clin Investig.* 2010;120:4289–302.
- Tang C, Lei X, Xiong L, Hu Z, Tang B. HMGA1B/2 transcriptionally activated-POU1F1 facilitates gastric carcinoma metastasis via CXCL12/CXCR4 axis-mediated macrophage polarization. *Cell Death Dis.* 2021;12:422.
- Gao Z, Xue K, Zhang L, Wei M. Over-Expression of POU Class 1 Homeobox 1 Transcription Factor (Pit-1) Predicts Poor Prognosis for Breast Cancer Patients. *Medical science monitor : international medical journal of experimental and clinical research.* 2016;22:4121–5.
- Huang YL, Chou WC, Hsiung CN, Hu LY, Chu HW, Shen CY. FGFR2 regulates Mre11 expression and double-strand break repair via the MEK-ERK-POU1F1 pathway in breast tumorigenesis. *Hum Mol Genet.* 2015;24:3506–17.
- De Paul AL, Gutierrez S, Sabatino ME, Mukdsi JH, Palmeri CM, Soaje M, et al. Epidermal growth factor induces a sexually dimorphic proliferative response of lactotroph cells through protein kinase C-ERK1/2-Pit-1 in vitro. *Exp Physiol.* 2011;96:226–39.
- Hunsaker TL, Jefferson HS, Morrison JK, Franklin AJ, Shewchuk BM. POU1F1-mediated activation of hGH-N by deoxyribonuclease I hypersensitive site II of the human growth hormone locus control region. *J Mol Biol.* 2012;415:29–45.
- Martinez-Ordonez A, Seoane S, Avila L, Eiro N, Macia M, Arias E, et al. POU1F1 transcription factor induces metabolic reprogramming and breast cancer progression via LDHA regulation. *Oncogene.* 2021;40:2725–40.
- Wei Y, Tongjiang X, Peng Q, Guangming X. Caveolin-1 promotes pituitary adenoma cells migration and invasion by regulating the interaction between EGR1 and KLF5. *Exp Cell Res.* 2018;367(1):7–14.

Publisher's Note

Springer Nature remains neutral with regard to jurisdictional claims in published maps and institutional affiliations.